Universidad de Concepción
Dirección de Postgrado
Facultad de Ingeniería -Programa de Magíster en Ciencias de la Ingeniería, Mención
Ingeniería Civil

# Socavación Local y Sedimentación alrededor de Cepas de Puente durante Crecidas

# (Local Scour and Deposition at Bridge Piers during Floods)

Tesis para optar al grado de Magíster en Ciencias de la Ingeniería con
mención en Ingeniería Civil

MARCELO JAVIER GARCÍA MEDEL
CONCEPCIÓN-CHILE
2018

Profesor Guía: Oscar Link Lazo
Dpto. de Ingeniería Civil, Facultad de Ingeniería
Universidad de Concepción

# ABSTRACT

A better understanding of the bridge pier scour caused by flood waves is expected to allow a different design approach based on the expected scour depth caused by one hydrological event in combination with appropriate monitoring and maintenance of pier foundations, having risk levels of comparable magnitude to the current approach, which considers a worst case scenario represented by the hundred years recurrence discharge over a theoretically infinite duration.

The present Thesis aims at investigating the effects of different flow and sediment regimes (regulated and unregulated discharges with or without excess sediment supply) on local scour at a bridge pier. Concurrent field measurements of maximum scour depth, flow depth, and flow velocity were performed during six days at the Rapel bridge, over the Rapel river, located in Central Chile. During the measurements, river discharge was regulated by the operation of a hydropower plant, with hydropeaking. A model of scour and deposition is proposed, and field measurements are used to estimate optimal model parameters and to evaluate model performance. The model was applied to pre and post-dam scenarios to compare expected scour caused by a natural flow regime and by hydropeaking considering different excess sediment supply.

Results show that a single measurement of scour evolution during one flood was enough for estimation of optimal model parameters. The calibrated model reproduced measured scour and deposition in a verification case with high precision. The model application showed that scour and deposition are very sensitive to the excess sediment supply: after two years, scour resulted higher in the pre-dam scenario than in the post-dam scenario when no sediment deposition or equilibrium conditions occurred, while it was lower in case of excess sediment supply. However, in the pre-dam scenario with excess sediment supply the highest scour depths were of comparable magnitude as those after the two years, and occurred only briefly around the peak discharges before sediment deposition, illustrating the complex interactions between flow and sediment in time, with important consequences for monitoring of bridge pier scour in the field and for forensic analyses.

# ACKNOWLEDGEMENTS

**CONTENTS**

## LIST OF TABLES

## LIST OF FIGURES

# CHAPTER 1        INTRODUCTION

## 1.1    Motivation

The problem to be investigated within this Thesis deals with the scour caused by flood waves at bridge. It is relevant because bridges represent a significant part of the Chilean public investment in infrastructure, and are part of the so-called lifelines systems. Worldwide scour is the number one cause of bridge failure and it occurs mostly during high water events, due to the action of flood waves. In Chile, there is no systematic information to state if scour is the main cause of bridge failures or not. However, in recent years some collapses attributed to scour occurred in Chile, like e.g. the Loncomilla bridge on November 18, 2004. During the winter of 2006, in June, several rivers and streams located in the Biobío Region of Chile presented extreme flood events with associated return periods about 70 to 150 years, depending on the specific site. The extreme high water event caused severe scour around many bridge foundations. During the flood, an important number of minor bridges failed. Thus, many of them have been replaced. As in many rivers around the world, those located in the Central-South part of Chile exhibit floods with durations significantly shorter than the time required to achieve the maximum scour depth. A preliminary estimation shows that time to reach equilibrium scour in a sand bedstream is in the order of 10 days, while floods durations in the VIII region of Chile rarely exceed 2 days.

Because of its relevance, bridge scour is a mainstream research theme in hydraulic engineering. Since the top-cited state-of-the-art paper by Breusers et al. (1977) the specialized literature offers a large number of papers on the topic. In recent years, scour research has focused on coherent structures dynamics and sediment motion at the scour hole, following experimental measurements and advanced numerical simulations, time-dependent scour prediction, scour of cohesive sediments, and countermeasures. Even when scour depth is a controlling design parameter of bridge piers, scour has been studied previously almost always in the laboratory, using sand as sediment material, and imposing steady state hydraulics, i.e., a constant discharge. According to design manuals expected scour is calculated for the maximum discharge associated to the one hundred year recurrence flood, assuming that peak flood discharge acts over a time as long as that required to achieve the complete development of the scour hole, called equilibrium

time. The following concerns might explain the important discrepancies that have been found between predicted and observed scour: (1) Available scour formulas were deduced from experiments with sediments that up-scaled to the real-scenario represent piers in very coarse sediment. (2) The flow-causing scour is assumed to be constant and long lasting, while peak flows during real floods last only a limited amount of time. (3) Velocities during the experiments are kept close to the critical velocity for initiation of sediment motion, while during real floods the critical velocity can easily be exceeded by 20 times or more leading to significant entrainment into suspension.

Recognizing that floods are characterized at least by their peak discharge, duration, and hydrograph shape, with all of these parameters obviously influencing scouring, the present Thesis will study scour under conditions closer to real cases than performed before in hydraulic engineering.

## 1.2    Hypothesis

The research hypothesis was sediment deposition during the falling limb of a flood diminish the local scour depth at bridge piers.

## 1.3    Objectives

### 1.3.1   General objective

The general objective is to investigate the effects of different flow and sediment regimes (regulated and unregulated discharges with or without excess sediment supply) on local scour at a bridge pier.

### 1.3.2   Specific objectives

Perform concurrent field measurements of scour and flow during floods at a real bridge pier.

Extend an existing time-dependent scour model to include the potential effects of sedimentation on the scour depth at bridge piers.

Analyze the scour evolution at bridge piers in rivers with different flow and sediment regimes (regulated and unregulated discharges with or without excess sediment supply).

## 1.4     Methodology

Scour and flow were measured at the Rapel bridge during six days in which six flood waves were produced by the operation of the Rapel hydropower plant. A mathematical model proposed by Link et al. (2017) was extended to include the effects of sedimentation on scour depth. Scour evolution at bridge piers in rivers was analyzed through computation of scenarios of 2-years duration, namely a pre and a post-dam scenario.

## 1.5     Structure of the thesis

Chapter 1 presents the general problem to be investigated, working hypothesis, and general and specific goals, as well as an outline of the methodology. Chapter 2 present a review of the main theories and techniques related to the analysis of field scour and floods at bridge piers. Chapter 3 describes the materials and methods, in particular the study site, measuring techniques and mathematical formulation of the proposed model extension. Chapter 4 present the main results of the investigation, including the analysis of scenarios of two years duration for a pre and a post dam case at Rapel bridge. Finally, Chapter 5 concludes with final remarks on the obtained results and ways to proceed forward.

**CHAPTER 2          STATE OF THE ART REVIEW**

**2.1      Introduction**

This Chapter presents a brief literature review on the field measurements and modelling of scour and deposition at bridge piers.

**2.2      Scour depth estimation**

Hydraulic design of bridges includes the estimation of expected scour at its foundations, i.e. piers and abutments, typically considering the maximum equilibrium scour depth. Bridge scour formulas are believed to be conservative (Sheppard et al. 2014; Qi et al. 2016), however scour is responsible for more than 50% of the bridge failures over the world (Brandimarte et al. 2012; Proske 2018). Uncertainty is in part attributed to the fact that scour formulas have been derived from laboratory experiments, introducing simplifications such as idealized channel and pier geometries, constant discharge, clearwater conditions, and uniform sediments (e.g.: Melville and Chiew 1999; Oliveto and Hager 2002; Tubaldi et al. 2017), which lead to important scale effects (Ettema et al. 1998, 2006; Heller 2011 2017; Link et al. 2018).

**2.3      Field measurements of bridge scour depth during floods**

A number of technologies for field monitoring of the pier scour are available (e.g. Walker and Hughes 2005; Yu and Yu 2010; Lueker et al. 2010; Briaud et al. 2011; Prendergast and Gavin 2014), such as sliding magnetic collars (Yankielun and Zabilansky 1999), numbered bricks (Lu et al. 2008), or sonars (Sturm et al. 2004; Clubley et al. 2015). However, field measurements of scour during floods are practically nonexistent, due to difficulties in accessibility to bridge foundations during high waters, sensors performance in turbid currents, damage of sensors by LWD, blockage of piers and sensors by LWD, etc. Up to date, time-dependent scour formulas cannot be calibrated/verified for real life conditions due to the lack of adequate field data.

Exceptions are the outstanding field measurements conducted in Taiwan during typhoons reported by Lu et al. (2008), Su and Lu (2013, 2016), and Hong et al. (2016). In particular, the refilling of the scour-hole due to the sediment deposition associated with a disbalance in time is a challenging issue for monitoring of bridge piers, scour modelling, and forensic analyses.

## 2.4    Conclusion

The literature review evidenced a lack of antecedents for an accurate description and full understanding of the time evolution of scour during a sequence of river floods.

**CHAPTER 3          MATERIALS AND METHODS**

## 3.1      Introduction

This Chapter presents the materials and method for the analysis of the time dependent bridge pier scour during floods waves considering local scour and deposition. Therefore, the study site, measuring techniques and mathematical model are presented in detail.

## 3.2      Study site

The Rapel bridge is located in the Rapel watershed (13,700 km$^2$) in central Chile (71°44'9" W, 33°56'22" S). The bridge was built in 1954 and has six elliptical piers spaced 30 m one from each other. In 1956, a 350 MW hydropower plant located 24 km upstream started its construction and began operations in 1968. Figure 3.1 shows the location of the Rapel watershed and river, as well as a scheme of the bridge cross section with estimated pre-dam bed level and in-situ measured scour.

Table 3.1 summarize the important properties of the bridge and study site, while Figure 3.2 shows the grain size distribution of the riverbed sediments at Rapel bridge cross section. The riverbed is unimodal, composed of non-uniform gravels with $d_{50} = 33.5$ mm, $d_{90} = 81.3$ mm, and a geometric standard deviation of the sediment grain sizes $\sigma = 2.2$.

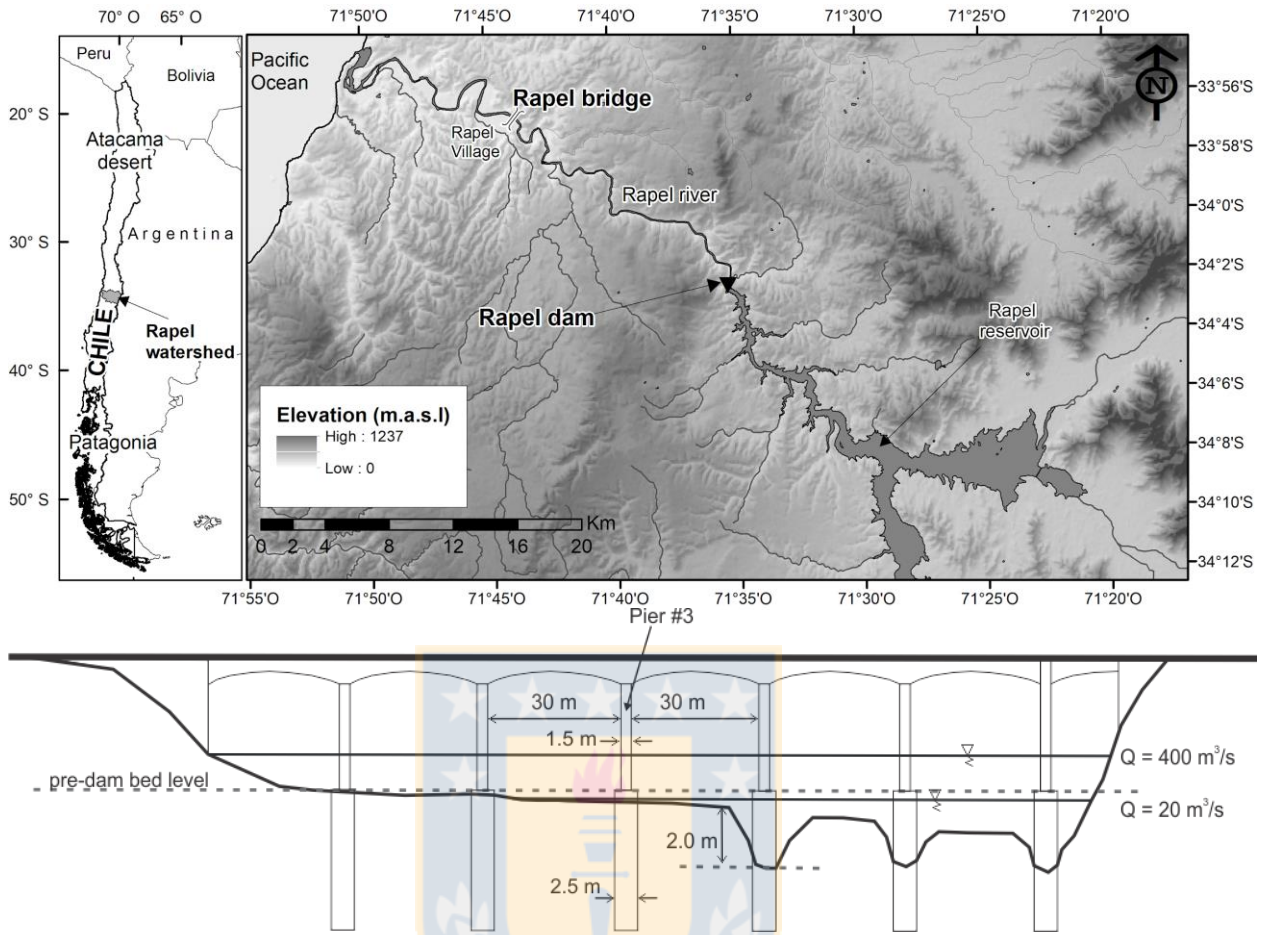Figure 3.1 Location of Rapel watershed, river and bridge (top) and scheme of the bridge cross section (bottom).

Table 3.1 Properties of the bridge and study site

| Property | Quantity |
|---|---|
| Bridge geometry | elliptical footing |
| Bridge length (m) | 220 |
| Number of piers | 6 |
| Bridge span (m) | 30 |
| Pier width (m) | 2.5 |
| Drainage area (km$^2$) | 13,700 |
| Channel slope | ~ 0.13% |
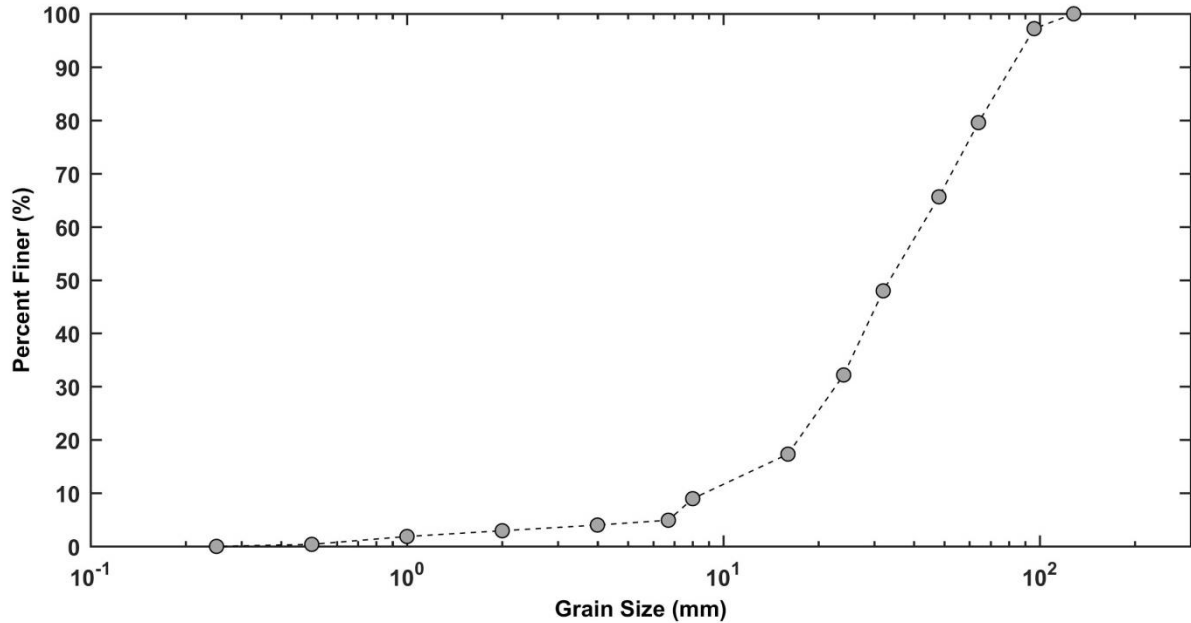
Figure 3.2 Grain size distribution of the riverbed sediments at Rapel bridge cross section

## 3.3    Measuring techniques

### 3.3.1    Streamflow

Streamflow data are available at the gauge station Rapel (administered by the National Water Agency of Chile) between 1939 and 1966. After 1966 the gauge station was dismantled. For the post-dam scenario, streamflow was computed from rating curves that were determined from flow depth and velocity measurements performed since 2016. Flow depth was measured using a pressure sensor (HOBO, U20-001-01) with a frequency of 10 minutes and a precision of ±0.5 cm. Discharge was measured using an acoustic Doppler current profiler (SonTek, RiverSurveyor M9). Additionally, measured data were interpolated and extrapolated using simulation results obtained with a 1D hydraulic model of the river reach built in Hec-Ras. Figure 3.3 shows the rating curves for the river at Rapel bridge.

For a given flow depth, the difference between rising and falling limb velocities was negligible, with maximum differences equal 0.06 m/s. In consequence, for scour computation flow velocity

was obtained from the rating curves in Figure 3.3. Figure 3.4 shows measured hydrographs before (April, 6th 1949 to April, 5th 1951) and after (April, 6th 2016 to April, 5th 2018) the dam operation. Periods were selected for analysis because they present a similar annual water volume 8.44 x $10^9$ and 5.67 x $10^9$ $m^3$, respectively.
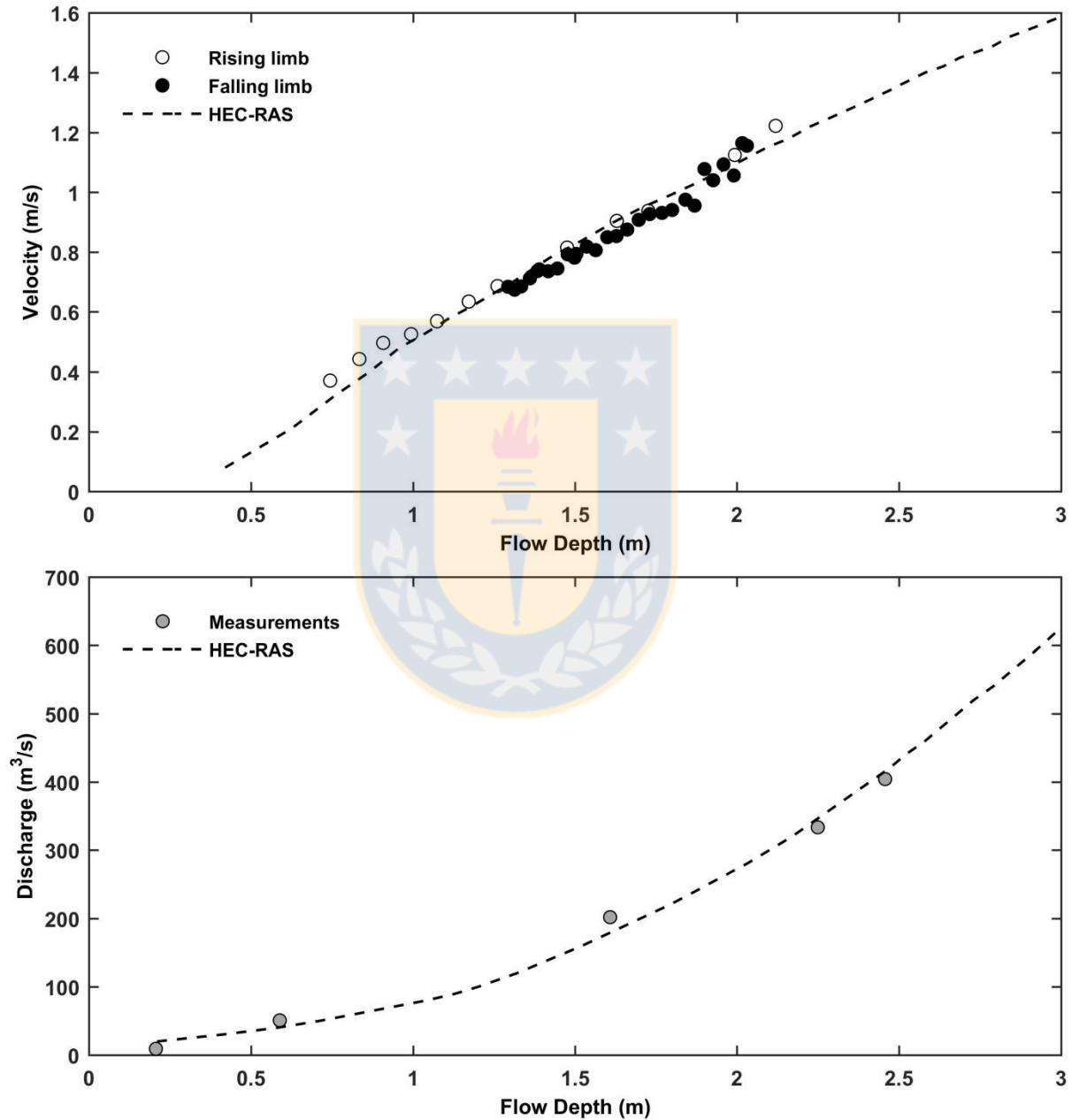


Figure 3.3 Rating curves at the bridge site
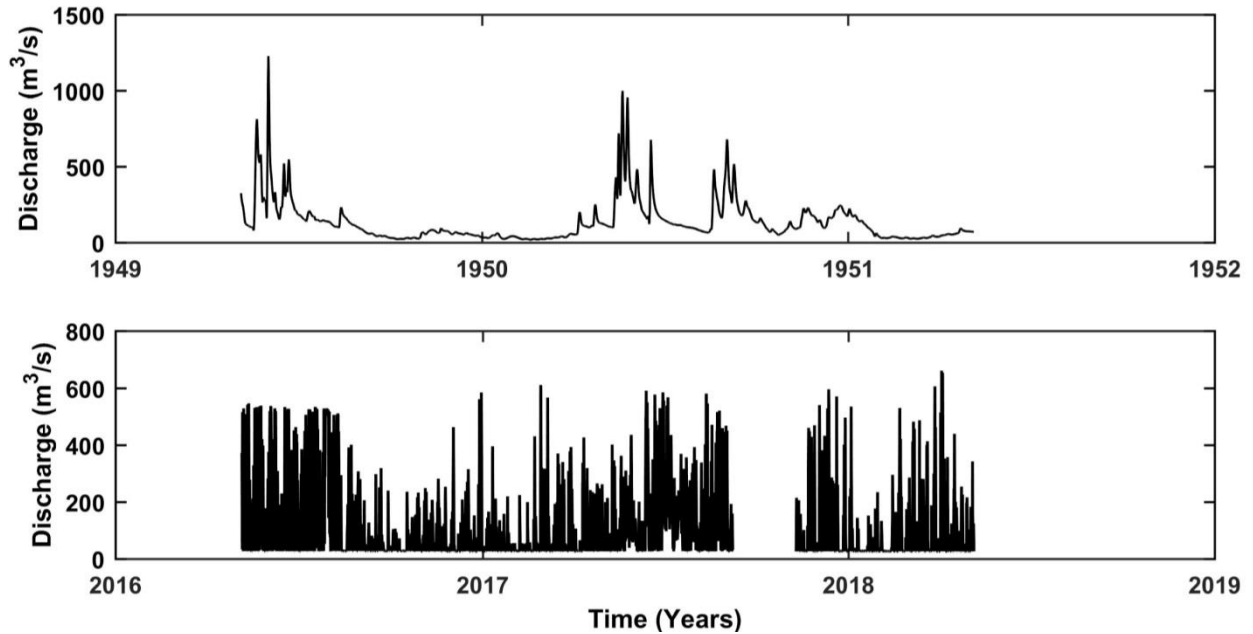
Figure 3.4 Pre (1941-1943) and post-dam (2016-2018) hydrographs

The pre-dam scenario represents an unregulated flow regime with discharges between 18 and 1230 $m^3$/s and marked seasonality, with low flows between October – March, and high flows between June and September. The post-dam scenario with daily hydropeaking represents a regulated flow regime with discharges varying between 20 and 660 $m^3$/s. Even when there are no sediment measurements available for these scenarios, the pre-dam case is presumed to have flood events with excess of sediment supply rate respect to the transport capacity as they are still common upstream the dam (Encina et al. 2006; Iribarren Anacona et al. 2015), while following Kondolf (1997), the post-dam scenario is presumed to have a sediment supply less or equal the transport capacity at a given instant.

### 3.3.2   Scouring

Scour at the front of Pier #3 of the Rapel bridge was measured with an ultrasonic scour sensor (Airmar, Echo Range SS510) having a frequency of 10 minutes and a precision of ±1 cm, which is equivalent to 0.3 times $d_{50}$. Figure 3.5 shows the Rapel bridge during low (a) and high (b)

flow, the installed scour sensor (c), the ADCP for velocity measurements (d), and the Helley-Smith measurements (e).
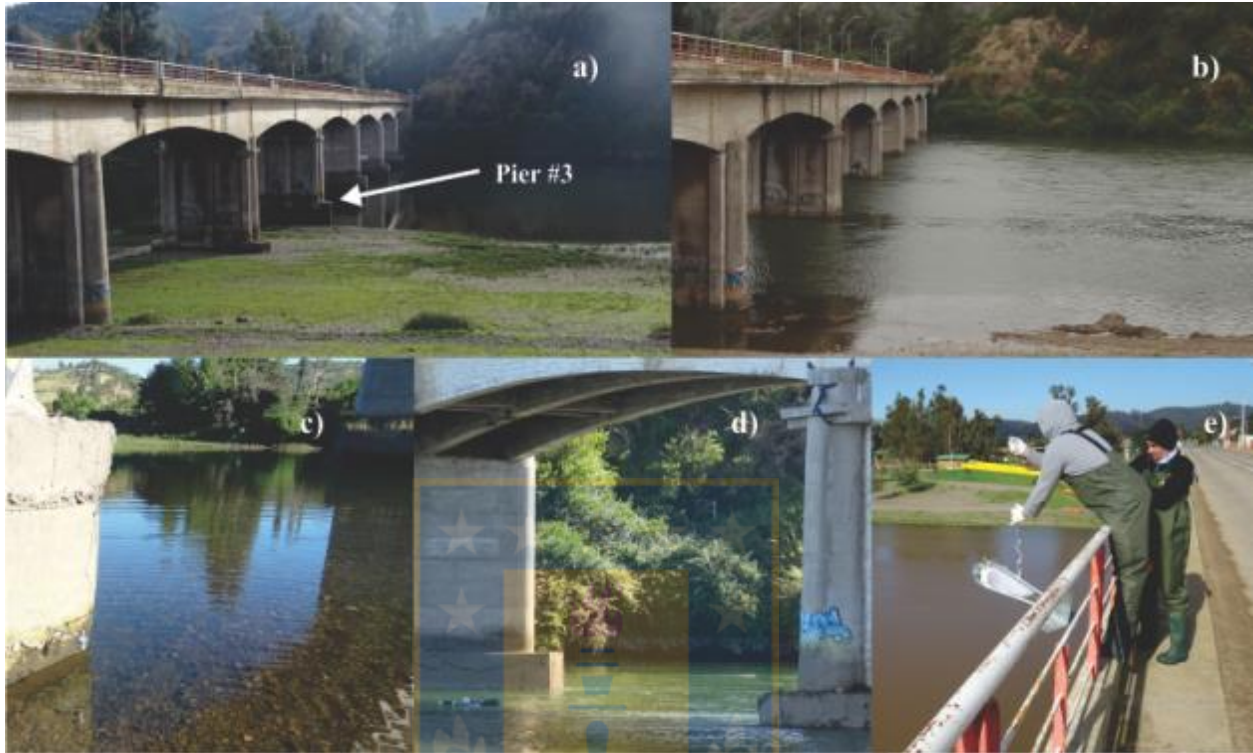


Figure 3.5 Rapel bridge during low flow (a), high flow (b), scour sensor at the front of Pier #3 (c), RiverSurveyor M9 ADCP mounted to a hydroboard (d), and bed-load sampling with Helley-Smith from the bridge deck (e)

## 3.4    Model framework

### 3.4.1   Bridge pier scour

The bridge pier scour in time was estimated with the DFW model, following Pizarro et al. (2017) and Link et al. (2017):

$$Z^* = c_1(1 - e^{-c_2 W^{*c_3}})$$                                                                (3.1)

where $Z^* = z/z_r$, z is the dimensional scour depth, $z_r = D^2/2d_s$ is a reference length, $D$ is the pier diameter, and $d_s$ is the representative sediment particle diameter, $c_1$, $c_2$, and $c_3$ are model parameters, and $W^*$ is the dimensionless effective flow work:

$$W^* = \int_0^{t_{end}} \frac{1}{t_c}\left(\frac{u_{ef}}{u_r}\right)^3 \delta dt \tag{3.2}$$

with

$$\delta = \begin{cases} 0 & u/u_{cs} < 0.5 \\ 1 & u/u_c \geq 0.5 \end{cases} \tag{3.3}$$

where $u$ is the section averaged flow velocity, $u_{cs}$ is the critical velocity for incipient scour, $u_{ef} = u - u_{cs}$ is the effective flow velocity, $u_c$ is the critical velocity for the initiation of sediment motion, $u_r = \sqrt{\rho' g d_s}$ is the reference velocity, $\rho' = (\rho_s - \rho)/\rho$ is the relative sediment density, $\rho_s$ is the sediment density, $\rho$ is the fluid density, $t_c = D^2/(2d_s u_{ef})$ is the characteristic time, $t_{end}$ is the considered time (e.g. hydrograph duration), The critical velocity for incipient sediment motion was computed with the Hjulström curve, approximated by Zanke's (1977) equation:

$$u_c = 1.4(\sqrt{\rho' g d_s} + 10.5\,{}^{\upsilon}\!/_{d_s}) \tag{3.4}$$

where $g$ is the acceleration of gravity and $\upsilon$ is the kinematic viscosity. Since the measurements are discrete on time, $W^*$ was computed in a discrete, approximate form as

$$W^* \approx \sum_{i=0}^{n} \frac{u_{ef}^4}{u_r^3 z_r} \delta \Delta t \tag{3.5}$$

with $n = t_{end}/\Delta t$, and $\Delta t$ the measuring interval of the unsteady discharge. $\Delta t$ was chosen as small as to allow a good resolution of the time variation of the variables in Eq. (3.5).


### 3.4.2   Sediment deposition at bridge piers

The sediment deposition, $Dep$, was computed following Foster and Huggins (1977) and Lu et al. (2008):

$$Dep = \int_0^{t_{end}} \frac{1}{\rho_s(1-p)} \alpha \frac{w_s}{q} (g_s - \beta g_s^*) dt \tag{3.6}$$

where $\alpha$ is a constant (= 0.5 according to Foster 1982 and Lu et al. 2008), $w_s$ is the sediment falling velocity (m/s) which was computed with the formula by Cheng (1997), $q$ is the specific discharge per unit width (m$^3$/m/s), $p$ is the riverbed porosity, $g_s$ is the sediment supply rate (kg/m/s), and $g_s^*$ is the sediment transport capacity (kg/m/s). $\beta$ is a correction factor introduced by Lu et al. (2008) which for the river Cho-Shui diminished with discharge from 8 to 2.5, as the Cho-Shui river presented a high sediment load, especially during typhoons. Note that Eq. (3.6) neglect the effects of discharge unsteadiness on sediment deposition, as the only contribution to deposition occur when the sediment supply exceeds the transport capacity at a given instant.

In this study, the sediment transport capacity was estimated through the fractional transport formulation by Dey (2014). The Meyer-Peter and Müller (1948) formula was used for computation of the bed-load capacity because it performs well for the Rapel river (Benitez, 1983), and thus $\beta = 1$. The sediment supply rate was computed as $g_s = \xi g_s^*$ with an excess sediment supply coefficient, $\xi \in [1, +\infty[$. Deposition occur (a) if the sediment supply rate is equal or greater than the transport capacity, i.e. when $\xi > 1$, which is expected to occur in unregulated rivers with flows caused by storms that typically produce an important sediment supply to the river through landslides and hillslope runoff, but also (b) if the sediment load exceeds the transport capacity due to a reduction of the latter in time, e.g. during the falling limb of the hydrograph, i.e. when $\xi g_s^{*t-\Delta t} > g_s^{*t}$, where $t$ is the time instant, and $(t - \Delta t)$ is a previous instant. To consider both deposition causes at Rapel bridge, sediment deposition over a time interval $\Delta t$ was computed as:

$$Dep \approx \begin{cases} 0 & , \quad \xi g_s^{*t-\Delta t} \le g_s^{*t} \\ \dfrac{\alpha w_s}{\rho_s(1-p)} \dfrac{\xi g_s^{*t-\Delta t} - g_s^{*t}}{q^t} \Delta t & , \quad \xi g_s^{*t-\Delta t} > g_s^{*t} \end{cases} \tag{3.7}$$

## 3.5    Estimation of model parameters and performance

The first parameter of the scour model, $c_1$, corresponds by definition to the equilibrium scour depth. It was computed with the scour formula proposed by Sheppard et al. (2014):

$$c_1 = Z_{eq}^* = Z_{eq}\left(\frac{2d_s}{D^2}\right) \tag{3.8}$$

$$\frac{Z_{eq}}{a^*} = 2.5 f_1 f_2 f_3 \qquad for\, 0.4 \leq \frac{u_1}{u_c} \leq 1.0 \tag{3.9}$$

$$f_1 = \tanh\left(\left(\frac{h}{a^*}\right)^{0.4}\right) \tag{3.10}$$

$$f_2 = \left\{1 - 1.2\left[\ln\left(\frac{u_1}{u_c}\right)\right]^2\right\} \tag{3.11}$$

$$f_3 = \left\{\frac{\left(\dfrac{a^*}{d_s}\right)}{0.4\left(\dfrac{a^*}{d_s}\right)^{1.2} + 10.6\left(\dfrac{a^*}{d_s}\right)^{-0.13}}\right\} \tag{3.12}$$

where $Z_{eq}$ is the equilibrium scour depth, $Z_{eq}^*$ is the dimensionless equilibrium scour depth, $d_s$ is the sediment size, $D$ is the pier diameter, $a^* = K_s a_p$ is the effective diameter of the pier, $h$ is the flow depth, $K_s$ is the shape factor, $a_p$ is the projected width of the pier, $u_1$ is average velocity in upstream main channel.

The parameters $c_2$ and $c_3$ were determined fitting the DFW model, i.e. Eq. (3.1), to concurrent measurements of discharge and scour depth, computing the dimensionless effective flow work $W^*$ and the relative scour depth $Z^*$ applying the Levenberg-Marquardt algorithm in Matlab®. $W_0^*$ and $\xi$ were obtained applying the genetic algorithm in Matlab® optimizing the root mean square error (RMSE). The quality of the model performance was determined through the RMSE and the Nash-Sutcliffe efficiency (NSE):

$$RMSE = \sqrt{\frac{1}{n}\sum_{i=1}^{n}\left(Z_i^{cal} - Z_i^{obs}\right)^2} \tag{3.13}$$

$$NSE = 1 - \left[\sum_{i=1}^{n}\frac{\left(Z_i^{obs} - Z_i^{cal}\right)^2}{\left(Z_i^{obs} - Z_i^{mean}\right)^2}\right] \tag{3.14}$$

where $Z_i^{cal}$ is the $i$th calculated value of scour, $Z_i^{obs}$ is the $i$th observed value of scour, $n$ is the number of observations, and $Z^{mean}$ is the mean value of the observed data.

Model parameters were estimated for two case studies with the aim to test the proposed formulation under different field conditions. Field data at Cornelia bridge over the Chattahoochee River were available for one flood occurred in July 1-2, 2003 documented by Sturm et al. (2004). An initial scour depth of 1.07 m was reported before beginning of the field measurements. Sediment deposition occurred after the peak discharge. Additionally, model parameters were estimated for the Rapel bridge using a single clear-water flood occurred in December, 7th 2017, and model performance was evaluated for estimation of scour evolution during five successive flood waves occurred in December, 8-12th 2017. Before field measurements the riverbed was flattened. Refilling of the scour hole was observed during the falling limb of the last measured flood.

Computed and observed scour depths over time were compared graphically and the quality of the computations was determined through the RMSE and NSE.

## 3.6    Model application for scour and deposition analysis at bridge piers

The calibrated model was applied to simulate scour at Rapel bridge, Pier #3, over a two-years period in a pre-dam (1949-1951) and a post-dam (2016-2018) scenario, considering different excess sediment supply. Scour and deposition in both scenarios were compared.

## 3.7    Conclusion

The methods for measurement and modelling of scour at bridge pier #3 of Rapel bridge were presented. Particularly, scour will be monitored with a scour sensor, and floods will be studied synoptically using an ADCP. The proposed mathematical model allows the analysis of scour in different flow and sedimentological regimes.

## CHAPTER 4          RESULTS

### 4.1     Introduction

This Chapter presents the main results from the field measurements and the computation of scenarios through the proposed mathematical model. Especial attention is given to the accuracy and quality of the measurements and computations.

### 4.2     Parameters estimation and model performance

#### 4.2.1   Cornelia bridge

Figure 4.1 shows the scour depth over time during a flood measured at the front of pier #1 of Cornelia bridge over the Chattahoochee river.

Scour progressed from the initial 1.07 m to 1.66 m measured during the peak and decreased to 1.12 m due to the sediment deposition during the falling limb of the hydrograph. The optimal model parameters for this case were $c_1 = 0.0028$, $c_2 = 0.0272$, $c_3 = 0.3014$, $\xi = 2.18$, and $W_0^* = 3.046*10^4$. The calibrated model (red continuous line) reproduced the measured scour depth with RMSE = 0.050 m and NSE = 0.93. The solid black line corresponds to the computed scour without considering deposition process, while the grey band provides a sensitivity of the computed scour depth to the $\xi$ parameter. Even when available data were not enough for a rigurous calibration and validation proccedure, obtained RMSE and NSE provide a good idea of the best performance that the proposed model could achieve.
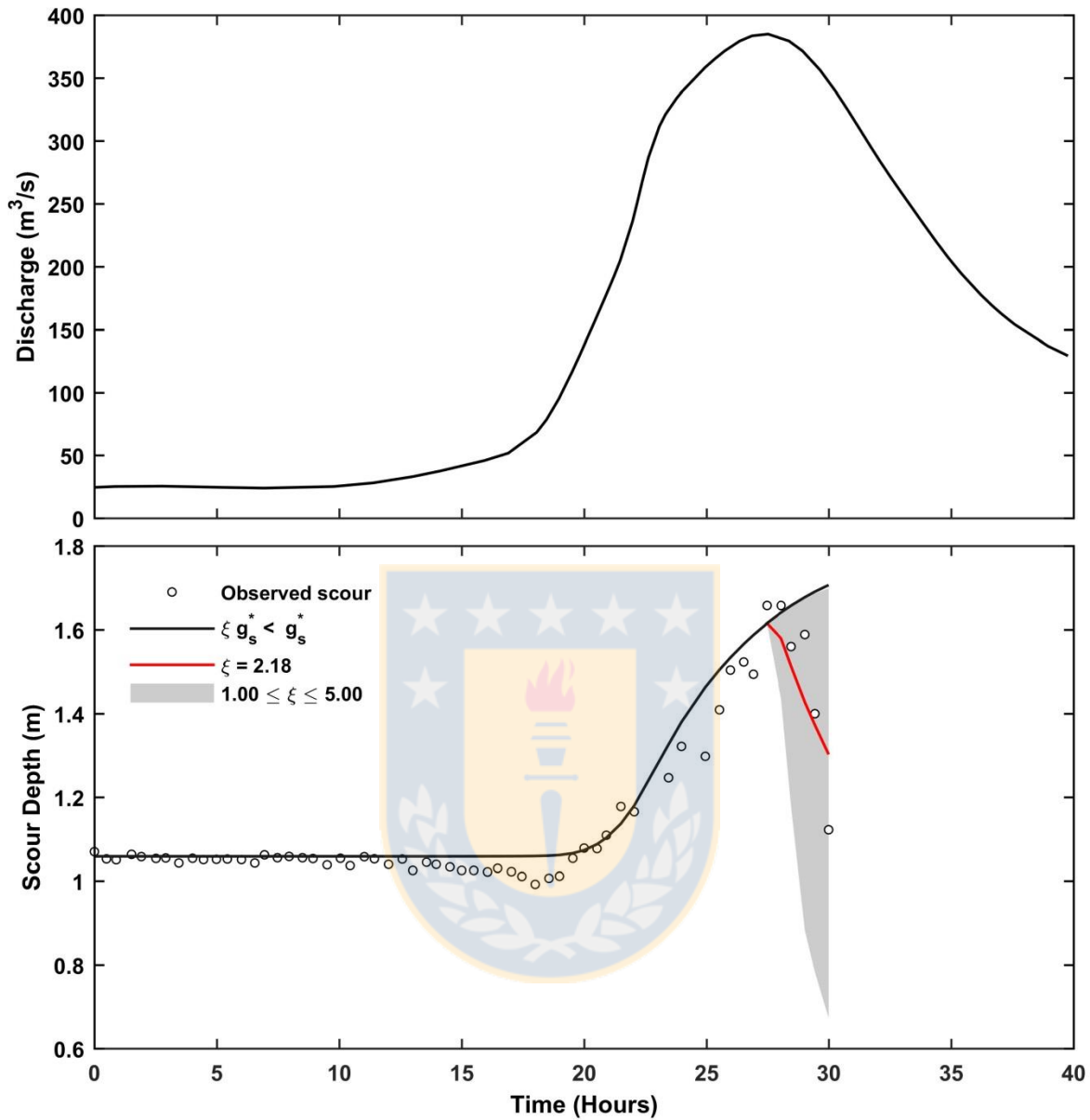
Figure 4.1 Scour depth over time during a flood measured at the front of Pier #1 of Cornelia bridge over the Chattahoochee river. The solid black line corresponds to the computed scour without deposition. The grey band around the calibrated model provides a sensitivity of the computed scour depth to $\xi$

### 4.2.2   Rapel bridge

Figure 4.2 shows the scour depth over time during 6 days with daily hydropeaking measured at the front of Pier #3 of Rapel bridge.



Figure 4.2 Scour depth over time during 6 days with daily hydropeaking measured at the front of Pier #3 of Rapel bridge. The grey band around the calibrated model provides a sensitivity of the computed scour depth to $\xi$

Observed scour increased from the initial flat bed to 0.48 m after 4.5 days. After the last flood peak (0.5 days), scour diminished 0.05 m due to sediment deposition. Estimation of optimal

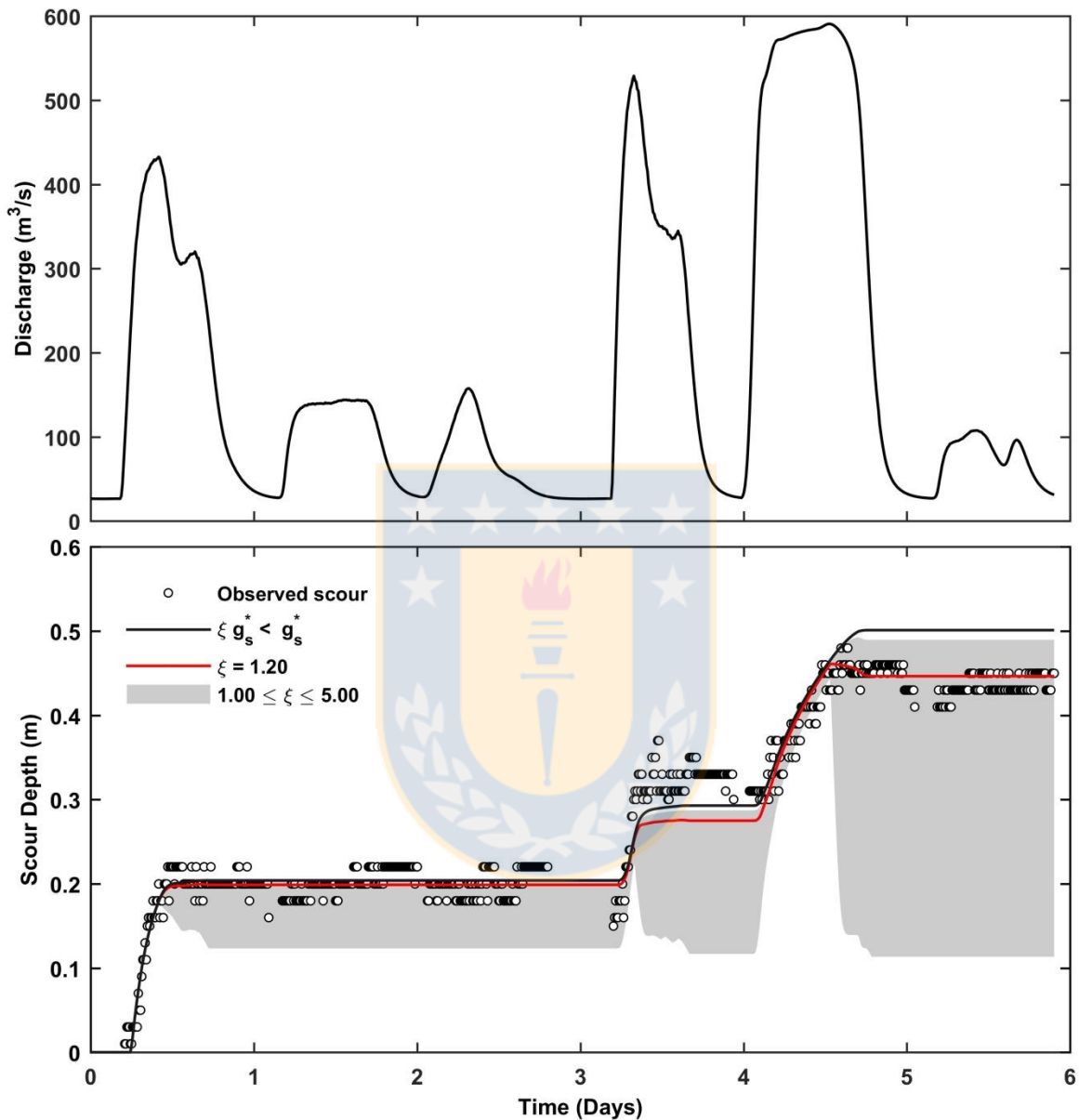parameters was performed using the first flood only (day 1). The optimal parameters were: $c_1 = 0.058$, $c_2 = 0.028$, $c_3 = 0.27$, and $\xi = 1.20$. The scour model alone (without sediment deposition, solid line) reproduced observed scour over days 2 to 5 with a RMSE = 0.036 m and NSE = 0.90. Results of the optimized model improved to RMSE = 0.025 m and NSE = 0.95. As for the Cornelia bridge model results for the Rapel bridge are considered very good for the estimation of scour and deposition during floods.

## 4.3 Scour and deposition at bridge piers during floods

Figure 4.3 shows computed scour depth over two years in the pre and post-dam scenarios, without sediment deposition ($\xi g_s^* < g_s^*$), with sediment supply equal transport capacity ($\xi = 1$), and with excess sediment supply ($\xi = 1.20$ and 5.00). Table 4.1 shows the computed maximum, average, and final scour depth at Pier#3 for both scenarios, under the different sediment regimes.

Table 4.1 Computed maximum, average, and final scour depth at Pier#3 for both scenarios, under the different sediment regimes

| Parameters | Pre dam | | | Post dam | | |
|---|---|---|---|---|---|---|
| | Z max (m) | Z avg (m) | Z end (m) | Z max (m) | Z avg (m) | Z end (m) |
| $\xi g_s^* < g_s^*$ | 1.56 | 1.40 | 1.56 | 1.11 | 0.98 | 1.11 |
| $\xi = 1.00$ | 1.39 | 1.27 | 1.38 | 0.84 | 0.79 | 0.80 |
| $\xi = 1.20$ | 0.97 | 0.40 | 0.34 | 0.60 | 0.50 | 0.52 |
| $\xi = 5.00$ | 0.95 | 0.02 | 0.00 | 0.35 | 0.11 | 0.11 |
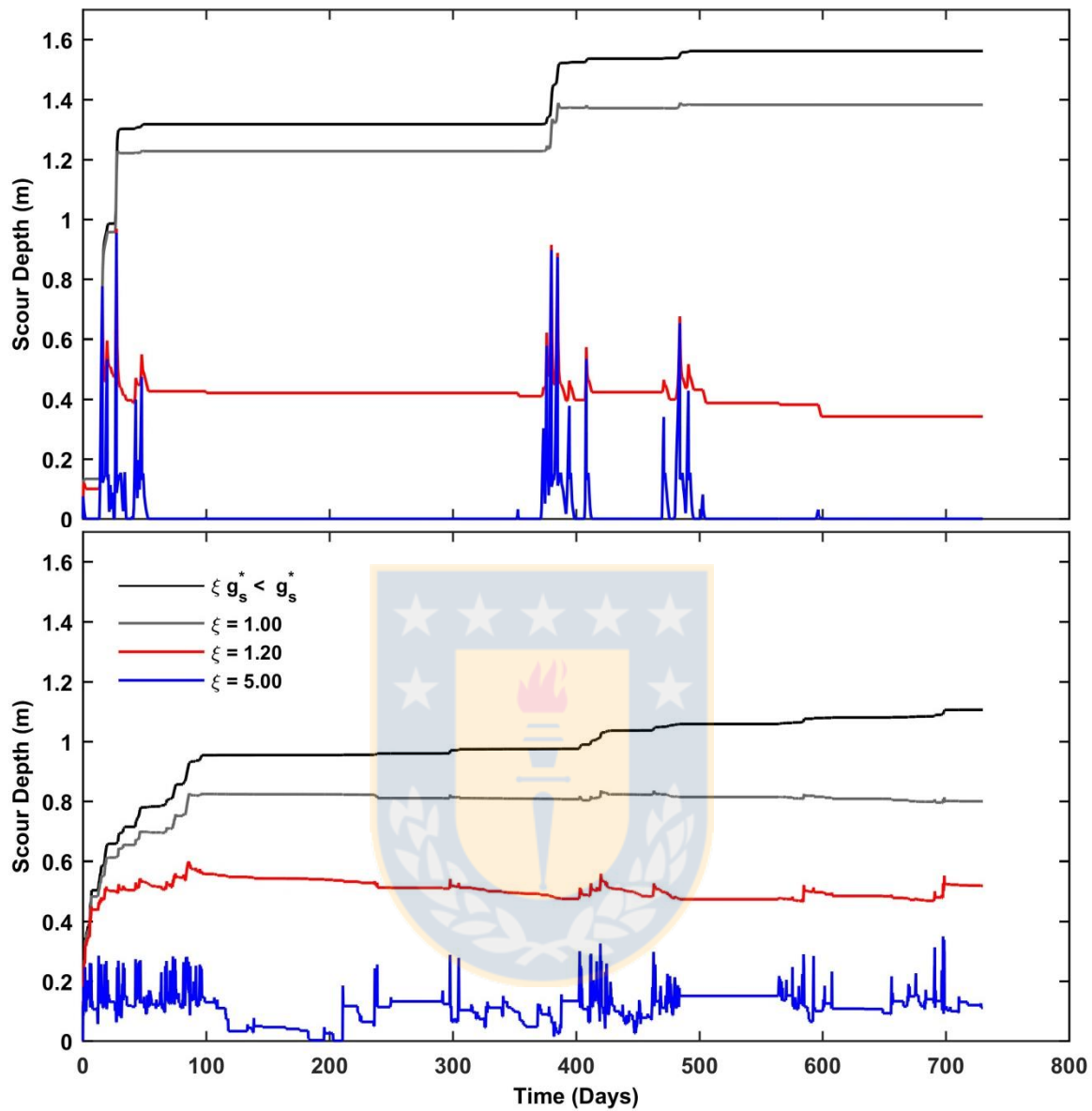
Figure 4.3 Computed scour depth over two years in a) the pre and b) the post-dam scenarios, without sediment deposition ($\xi g_s^* < g_s^*$, black line), with sediment supply equal transport capacity ($\xi = 1.00$, grey line), and with sediment supply excess of 20% ($\xi = 1.20$, red line) and 500% ($\xi = 5.00$, blue line)

Salient differences in scour depth appear as consequence of the different flow regimes: for scenarios without sediment deposition ($\xi g_s^* < g_s^*$) and equilibrium conditions ($\xi = 1.00$) the scour depth after the two years is higher in the pre-dam scenario than in the post-dam scenario,

while it was lower in cases with excess sediment supply ($\xi > 1.00$). Especially, in the pre-dam scenario with excess sediment supply scour depth reached high values during short periods of high waters (e.g. around 380 and 490 days), rapidly diminishing during the falling limb of the hydrographs due to sediment deposition. The latter is more marked for higher sediment supply, i.e. $\xi = 5.00$. This aspect has important consequences for bridge monitoring and forensic analyses: when sediment deposition is expected to occur, a bridge inspection after a flood will not provide adequate information about the maximum scour depth reached during the event. Therefore, an appropriate monitoring system able to work under high turbidity during floods is required.

## 4.4    Conclusion

Field measurements were performed over six days at Rapel bridge. They were used for calibration of a simple mathematical model. The model was applied for analysis of time dependent scour in scenarios with 2 years duration, considering different flow and sediment regimes. A high sensitivity of the local scour depth to the excess of sediment supply, $\xi$. Deposition played an important role in cases with $\xi > 1.0$, which are expected to frequently occur.
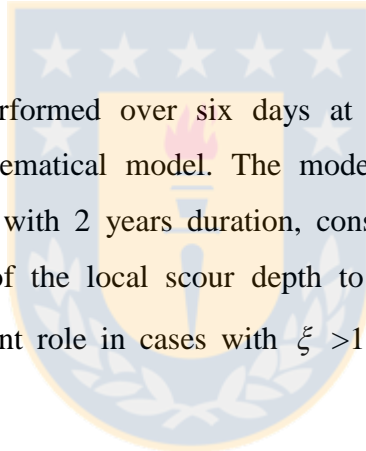
**CHAPTER 5         CONCLUSIONS**

The effects of different flow and sediment regimes on pier scour were investigated through field measurements and computations with a simple scour-deposition model. The scour model was previously proposed by Link et al. (2017), while its extension for modelling the sediment deposition was proposed in the present Thesis.

The ultrasonic scour sensor was a reliable instrument for real scour monitoring under the presented field conditions, and results show that a single and easy-to-perform measurement of scour evolution during one flood is enough for estimation of optimal model parameters. The field measurement of scour is especially challenging due to a number of unresolved issues, such as the potential damage and blockage of the sensor by large woody debris, the water turbidity that at a certain point would avoid the measurement of the river bottom, the access to the river during floods which can be dangerous for instruments operators. The presented field conditions were relatively simple, in comparison to other expected scenarios, especially in unregulated and mountain rivers, as those massively existing in Chile. Therefore, the presented measuring methodology must be taken with some care, and its application to different conditions needs a site-specific analysis of possible operational troubles.

The application of the proposed model showed that scour depth and deposition at a bridge pier are very sensitive to the excess sediment supply. In particular, after two years, scour in a pre-dam scenario (natural flow regime) resulted higher than in a post-dam scenario (regulated flow regime with daily hydropeaking) when no sediment deposition or equilibrium conditions occurred, while it was lower in case of excess sediment supply. The excess sediment supply is by definition a number that reflects riverflows overloaded by sediments. It is distinguished between the classical Newtonian water flow with sediment concentrations that are not able to alter the rheology, i.e. volumetric sediment concentration less than about 20%, hyperconcentrated flows where the flow exhibit already a different rheology than clear-water, and debris flow which is actually more sediment than water, with volumetric sediment concentrations of more than about 40% with a highly complex mechanical and dynamical behavior. In the present investigation, the value of the excess sediment supply parameter was varied from 1 to 5. Even when 5 is a high number, it must

be noted that it correspond to a sediment concentration well beyond the limit for hyperconcentrated flow. Thus, the presented analysis is valid only for river floods.

Remarkably, the highest scour depths in the pre-dam scenario with excess sediment supply were of comparable magnitude as those computed for a post-dam scenario, and occurred only briefly around the peak discharges before sediment deposition, illustrating the complex interactions between flow and sediment in time. This aspect have important consequences for instrumentation, monitoring and analysis of scour. Especially, monitoring of bridge pier scour in the field and forensic analyses needs to take flow and sediment regimes into account. Especial requirements for a continuous monitoring during floods arise in case of excess sediment supply. Otherwise, the maximum scour depth could be importantly underestimated.

A possible way forward would be to extend the present study with field measurements at a different bridge, with more marked sediment deposition, and to include the present modelling approach into a risk-based design procedure.
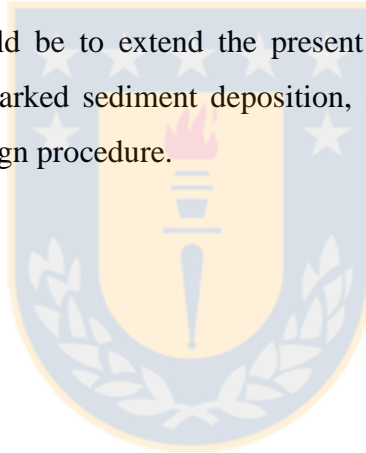
# REFERENCES

Benitez, A. (1983). Estimación del Gasto Sólido Afluente y del Embanque Producido en el Embalse de la Central Rapel Durante el Periodo de 11 Años 01/04/68-31/03/79. **Proceedings 6th National Congress Chilean of Society of Hydraulic Engineering**. Santiago. November.

Brandimarte, L., P. Paron and G. Di Baldassarre (2012) Bridge pier scour: A review of processes, measurements and estimates. **Environmental Engineering Management Journal, 11(5)**. 975-989.

Breusers, H., G. Nicollet and H. Shen (1977) Local scour around cylindrical piers. **Journal of Hydraulic Research, 15 (3).** 211-252.

Briaud, J.-L., S. Hurlebaus, K.A. Chang, C. Yao, H. Sharma, O. Y. Yu, C. Darby, B. E. Hunt and G. R Price (2011) **Realtime Monitoring of Bridge Scour Using Remote Monitoring Technology**. Texas Dept. of Transportation, Austin.

Cheng, N. (1997) Simplified settling velocity formula for sediment particle. **Journal of Hydraulic Engineering, 123(2)**. 149–152.

Clubley, S., C. Manes and D. Richards (2015) High-resolution sonars set to revolutionise bridge scour inspections. **Proceedings of the Institution of Civil Engineers, 168(1)**. 35–42.

Dey, S. (2014) **Fluvial Hydrodynamics: Hydrodynamic and Sediment Transport Phenomena**. Springer. Berlin.

Encinas, A., V. Maksaev, L. Pinto, J. P. Le Roux, F. Munizaga and M. Zentilli (2006) Pliocene lahar deposits in the Coastal Cordillera of central Chile: Implications for uplift, avalanche deposits, and porphyry copper systems in the Main Andean Cordillera. **Journal of South American Earth Sciences, 20(4)**. 369–381.

Ettema, R., G. Kirkil and M. Muste (2006) Similitude of large-scale turbulence in experiments on local scour at cylinders. **Journal of Hydraulic Engineering, 132:1**. 33-40.

Ettema, R., B. Melville and B. Barkdoll (1998) Scale effect in pier-scour experiments. **Journal of Hydraulic Engineering, 124(6)**. 639-642.

Foster, G. R. (1982) Modelling the erosion process. In Haan, C.T., H. P. Johnson and D. L. Brakensiej (eds.). **Hydrologic Modeling of Small Watersheds**, ASAE Monograph No. 5, ASAE, St., Joseph, Mich., 297-382.

Foster, G. R. and L. F. Huggins (1977) Deposition of sediment by overland flow on concave slopes. **Special publication No., 21, soil erosion prediction and control, Soil Conservation Society of America, Ankeny**, Iowa, 167-182.

Heller, V. (2011) Scale effects in physical hydraulic engineering models. **Journal of Hydraulic Research, 49(3)**. 293–306.

Heller, V. (2017) Self-similarity and Reynolds number invariance in Froude modelling. **Journal of Hydraulic Research, 55(3).** 293–309.

Hong, J.H., W.-D. Guo, Y.-M. Chiew and C.-H. Chen (2016) A new practical method to simulate flood-induced bridge pier scour – A case of study of Mingchu bridge piers on the Cho-Shui river. **Water, 8(6)**. 238.

Iribarren Anacona, P., A. Mackintosh, and K. P. Norton (2015) Hazardous processes and events from glacier and permafrost areas: Lessons from the Chilean and Argentinean Andes. **Earth Surface Processes and Landforms, 40(1)**. 2–21.

Kondolf, G. M. (1997) PROFILE: Hungry water: Effects of dams and gravel mining on river channels. **Environmental Management, 21(4)**. 533–551.

Link, O., C. Castillo, A. Pizarro, A. Rojas, B. Ettmer, C. Escauriaza and S. Manfreda (2017) A model of bridge pier scour during flood waves. **Journal of Hydraulic Research, 55(3)**. 310–323.

Link, O., S. Henríquez and B. Ettmer (2018) Physical scale modelling of scour around bridge piers. **Journal of Hydraulic Research**.

Lu, J.-Y., J.-H. Hong, C.-C. Su, C.-Y. Wang and J.-S. Lai (2008) Field measurements and simulation of bridge scour depth variations during floods. **Journal of Hydraulic Engineering, 134(6)**. 810-821.

Lueker, M., J. Marr, C. Ellis, A. Hendrickson and V. Winsted (2010) Bridge scour monitoring technologies: development of evaluation and selection protocols for application on river bridges in Minnesota. **Proceedings 5th International Conference on Scour and Erosion**. San Francisco. United States of America. November.

MathWorks (2017) **MATLAB Release 2017b** [Computer software]. The MathWorks Inc. Massachusetts.

Melville, B. and Y.- M. Chiew (1999) Time scale for local scour at bridge piers. **Journal of Hydraulic Engineering, 125(1)**. 59–65.

Melville, B. and S. Coleman (2000) **Bridge Scour**. Water Resources Publications. Littleton.

Meyer-Peter, E. and R. Müller (1948) Formulas for bed-load transport. **Proceedings 2nd Meeting of the International Association for Hydraulic Research**. Stockholm, Sweden. June.

Oliveto, G. and W. Hager (2002) Temporal evolution of clear-water pier and abutment scour. **Journal of Hydraulic Engineering, 128(:9)**. 811-820.

Pizarro, A., B. Ettmer, S. Manfreda, A. Rojas and O. Link (2017) Dimensionless effective flow work for estimation of pier scour caused by flood waves. **Journal of Hydraulic Engineering, 143(7)**.

Pizarro, A., C. Samela, M. Fiorentino, O. Link and S. Manfreda (2017) BRISENT: An entropy-based model for bridge-pier scour estimation under complex hydraulic scenarios. **Water, 9(11)**.

Prendergast, L. and K. Gavin (2014) A review of bridge scour monitoring techniques. **Journal of Rock Mechanics and Geotechnical Engineering, 6(2)**, 138–149.

Proske, D. (2018). **Bridge Collapse Frequencies versus Failure Probabilities**. Springer. Vienna.

Qi, M. J. Li and Q. Chen (2016) Comparison of existing equations for local scour at bridge piers: parameter influence and validation. **Natural Hazards, 82(3)**. 2089–2105.

Sheppard, D., B. Melville and H. Demir (2014) Evaluation of existing equations for local scour at bridge piers. **Journal of Hydraulic Engineering, 140(1)**. 14–23.

Sturm, T., F. Sotiropoulos, M. Landers, T. Gotvald, S. Lee, L. Ge, R. Navarro and C. Escauriaza (2004) **Laboratory and 3D Numerical Modeling with Field Monitoring of Regional Bridge Scour in Georgia**. Georgia Department of Transportation. Atlanta.

Su, C.-C. and J.-Y. Lu (2013) Measurements and prediction of typhoon-induced short-term general scours in intermittent rivers. **Natural Hazards, 66(2)**. 671–687.

Su, C.-C. and J.-Y. Lu (2016) Comparison of sediment load and riverbed scour during floods for gravel-bed and sand-bed reaches of intermittent rivers: Case study. **Journal of Hydraulic Engineering, 142(5)**.

Tubaldi, E., L. Macorini, B. A. Izzuddin, C. Manes and F. Laio (2017) A framework for probabilistic assessment of clear-water scour around bridge piers. **Structural Safety, 69**. 11–22.

Walker, J. F. and P. E. Hughes (2005) **Bridge Scour Monitoring Methods at Three Sites in Wisconsin**. U.S. Geological Survey, Reston.

Yankielun, N. E. and L. Zabilansky (1999) Laboratory investigation of time-domain reflectometry system for monitoring bridge scour. **Journal of Hydraulic Engineering, 125(12)**. 1279–1284.

Yu, X. B. and X. Yu (2010) **Field Monitoring of Scour Critical Bridges : A Pilot Study of Time Domain Reflectometry Real Time Automatic Bridge Scour Monitoring System**. Ohio Department of Transportation. Columbus.

Zanke, U. (1977). **Neuer Ansatz zur Berechnung des Transportbeginns von Sedimenten unter Stromungseinfluss**. Technical University Hannover. Hannover.